Assessment of bone synthetic activity in inflammatory lesions and syndesmophytes in patients with ankylosing spondylitis: the potential role of 18F-fluoride positron emission tomography-magnetic resonance imaging

S.-G. Lee[1], I.-J. Kim[1,2], K.-Y. Kim[3], H.-Y. Kim[2], K.-J. Pak[2], S.-J. Kim[2], E.-K. Park[1], Y.-K. Jeon[1], B.-Y. Yang[1], G.-T. Kim[4]

[1]Department of Internal Medicine, and [2]Department of Nuclear Medicine, Pusan National University School of Medicine, Pusan National University Hospital, Busan, South Korea; [3]Department of Nuclear Medicine and [4]Division of Rheumatology, Department of Internal Medicine, Kosin University College of Medicine, Busan, South Korea.

Abstract

Objective

18F-fluoride uptake represents active osteoblastic bone synthesis. We assessed bone synthetic activity in inflammatory lesions and syndesmophytes in patients with ankylosing spondylitis (AS) using 18F-fluoride positron emission tomography-magnetic resonance imaging (PET-MRI, Philips Healthcare, Cleveland, OH, USA) and x-ray.

Methods

All images of 12 AS patients were recorded with the presence or absence of increased 18F-fluoride uptake lesions on PET, acute (type A) or advanced (type B) corner inflammatory lesions (CILs) on MRI, syndesmophytes on x-ray at the anterior vertebral corners. An increased 18F-fluoride uptake lesion was defined as an uptake which is greater than the uptake in the adjacent normal vertebral body. The association of a CIL or syndesmophyte with an increased 18F-fluoride uptake lesion was investigated by generalised linear latent mixed models analysis to adjust within-patient dependence for total numbers of vertebral corners.

Results

There were 67 type A CILs (12.1%), 37 type B CILs (6.7%) and 58 increased 18F-fluoride uptake lesion (10.4%) out of 552 vertebral corners and there were 57 syndesmophytes (19.8%) out of 288 vertebral corners. A type A CIL (OR=3.2, 95% CI=1.6-6.5, p=0.001), type B CIL (OR=59.9, 95% CI=23.5-151.5, p<0.001) and syndesmpophyte (OR=21.8, 95% CI=5.5-85.2, p<0.001) were significantly associated with an increased 18F-fluoride uptake lesion.

Conclusion

Our data suggest that an inflammatory lesion as well as a syndesmophyte is associated with active bone synthesis assessed by 18F-fluoride uptake in the spine of AS patients. 18F-fluoride PET-MRI may have the potential for investigating the pathogenesis of structural damage in AS.

Key words

ankylosing spondylitis, positron emission tomography, fluoride, osteoblast

Seung-Geun Lee, MD
In-Joo Kim, MD, PhD
Keun-Young Kim, MD
Hee-Young Kim, MD
Kyoung-June Pak, MD
Seong-Jang Kim, MD, PhD
Eun-Kyoung Park, MD
Yun-Kyung Jeon, MD
Byeong-Yun Yang, MD
Geun-Tae Kim, MD, PhD

Please address correspondence to:
Dr In-Joo Kim,
Department of Internal Medicine,
Pusan National University
School of Medicine,
Pusan National University Hospital,
179 Gudeok-Ro,
Seo-Gu, 602-739 Busan,
South Korea.
E-mail: injkim@pusan.ac.kr

Received on July 3, 2014; accepted in revised form on September 17, 2014.

Competing interests: none declared.

Introduction

Ankylosing spondylitis (AS) is a chronic rheumatic disease that primarily involves inflammation of the axial skeleton, particularly the sacroiliac joints and the spine. A hallmark histopathologic feature of the disease is structural damage caused by excessive new bone formation in the form of syndesmophytes and spinal ankylosis. Although reparative processes that respond to inflammation may cause new bone formation, the pathogenesis underlying the structural damage in AS remains poorly understood. Specifically, previous results from several clinical trials report that tumour necrosis factor-α (TNF-α) blockers do not prevent structural damage even after spinal inflammation reduces dramatically, which raises a question about the relationship between inflammation and new bone formation in AS patients (1-3). Additionally, previous studies have shown that syndesmophytes developed vertebral edges with inflammation more frequently as compared to those without inflammation, but some studies have shown that new syndesmophytes can also develop in the absence of spinal inflammation (4-6). Thus, spinal inflammation and new bone formation are considered "uncoupled" or "disconnected" in the temporospatial manner, but this notion still remains controversial (7-9).

Imaging techniques are important for investigating the relationship between inflammation and structural damage in AS. New bone formation is best assessed by conventional radiography whereas fat suppressed magnetic resonance imaging (MRI) is currently recognised as the standard and reliable imaging modality for evaluating spinal inflammation in AS patients (10, 11). However, these 2 imaging tools have some limitations. First, low levels of histopathologic spinal inflammation are not detected by MRI (12). Second, structural damage in the thoracic vertebrae are not easily detected on conventional radiographs due to the overlying lung tissue (13). Moreover, these imaging modalities do not allow the visualisation of bone turnover.

However, 18F-fluoride labelled positron emission tomography (PET) scan is a useful technique for evaluating bone metabolism in both benign and malignant skeletal diseases with higher sensitivity and specificity than conventional 99mTc labelled phosphate and diphosphonate scans (14). Particularly, 18F-fluoride uptake represents active osteoblastic bone synthesis in both animal (15) and human studies (16, 17). Therefore, we suppose the 18F-fluoride PET scan has the potential to detect new bone formation in patients with AS.

In the present study, we investigated inflammatory changes and structural damage in the whole spines of AS patients using 18F-fluoride PET-MRI scan and conventional radiography. Subsequently, we assessed bone synthetic activity using 18F-fluoride tracer uptake in corner inflammatory lesions (CILs) on MRI and syndesmophytes on radiography.

Materials and methods

Study population

We prospectively recruited 12 male patients with AS and one male healthy volunteer from a university-affiliated rheumatology centre in South Korea from March 2013 to December 2013. All patients with AS were biologics-naïve and they fulfilled the modified New York criteria for AS (18). Exclusion criteria were 1) patients with rheumatic diseases other than AS; 2) on-going or previous therapy with calcium, vitamin D, bisphosphonate and other medications that can affect bone synthesis and resorption except for non-steroidal anti-inflammatory drugs (NSAIDs) and disease modifying anti-rheumatic drugs; 3) prior spine surgery or metal implants; 4) contraindications for MRI; 5) refusal to participate in the study. The healthy volunteer had no history of any musculoskeletal diseases and was not taking any medications for bone metabolism. Written informed consent based on the Helsinki Declaration was obtained from all subjects. This study was approved by the Research and Ethical Review Board of the Pusan National University Hospital in Busan, South Korea (H-1211-016-006).

Clinical and laboratory assessment

At the baseline visit, the clinical parameters including the Bath Ankylos-

ing Spondylitis Disease Activity Index (BASDAI), Bath Ankylosing Spondylitis Functional Index (BASFI) and Bath Ankylosing Spondylitis Metrology Index (BASMI) were measured and blood samples from all participants were taken to determine levels of C-reactive protein (CRP) and erythrocyte sedimentation rate (ESR). CRP levels were measured using particle-enhanced immunoturbidimetric assay (Tinaquant C-reactive protein, Roche Diagnostics, Switzerland) and an automated analyser the P-800 Modular (Roche, Switzerland).

Imaging protocol

The 18F-fluoride PET-MRIs of the whole spines were performed by using the Philips Ingenuity TF sequential whole-body PET/MR system (Philips Healthcare, Cleveland, OH, USA). The PET/MR system combines the Philips GEMINI TF PET camera and the Philips Achieva 3.0T X-series MRI system with a rotating bed that allows accurately registered sequential acquisition of MR and PET images. One hour after injection of a 222-296 MBq dose of 18F-fluoride, the patients were placed on the PET-MRI scanner bed and then the scanning was started. Emission scan time per bed position was 3 min; the scans were acquired in 9 bed positions. PET data were obtained using a high-resolution whole body scanner with an axial field of view (FOV) of 18cm. The average axial resolution varied between 4.2mm full width at half maximum in the centre and 5.6 mm at 10 cm. After scatter and decay correction, the PET data were reconstructed iteratively with attenuation correction and reoriented in the axial, sagittal, and coronal slices. The row action maximum likelihood algorithm was used for 3-dimensional reconstruction. The MRI sequence to correct PET attenuation was performed. It was followed by the coronal and sagittal T1-weighted and short tau inversion recovery (STIR) sequences of the entire spine. The whole spine MRI was performed using a 3T MRI unit, which was equipped with dual coil, 16 independent radiofrequency channels of neurovascular coil and 15 independent radiofrequencies of spine coil. Coronal T1-weighted spin-echo (repetition time [TR]/echo time [TE], 424/7.0 ms) and STIR (TR/TE/ inversion time [TI] 4158/70/230 ms) sequences of the total spines were acquired with a 3-station approach. The FOV (mm) of each station was 280×220. The matrix size was 228×220 for T1W1 and 288×213 for the STIR sequence. Total-spine coronal images were acquired with a 5-mm slice thickness for each sequence. Sagittal T1-weighted spin-echo (TR/TE, 400/7.4ms) and STIR sequence (TR/TE/ TI 2995/70/230 ms) were imaged with a three-station approach. The FOV of each station was 277×220. The matrix size was 342×276 for T1W1 and 180×220 for the STIR sequence. Total-spine sagittal images were acquired with a 4-mm slice thickness for each sequence. The 18F-fluoride PET-MRIs of PET/MR system took approximately 90 minutes to perform and provided flawless image quality without apparent artifacts and technical failures. In addition, lateral views of the cervical and lumbar spine using conventional radiography were also obtained the same day of the 18-fluoride PET-MRI scanning.

Definition of a spinal lesion in the imaging modalities

According to the standardised definition for spinal lesions by the developed international working group of rheumatologists and radiologists from Canada and Denmark (19), a CIL is defined as an increased STIR signal at the anterior vertebral corner on at least one sagittal slice on MRI. A CIL is further categorised as "Type B" or a "dimorphic" CIL if the increased signal on STIR has partially receded from the vertebral corner, but this lesion extends to both the vertebral endplate and the anterior or posterior border of the vertebral body adjacent to the corner, (Fig. 1) (19, 20). On the contrary, the inflammatory signal extends completely to the anterior corner in "type A" CIL (Fig. 1) (19, 20). Type A CIL represents an early inflammatory process whereas type B CIL reflects more advanced reparative lesion associated with tissue metaplasia (19, 20). Increased 18F-fluoride uptake lesion was defined as an uptake which is greater than that in the adjacent normal vertebral body. Both CILs and increased 18F-fluoride uptake lesion were evaluated on the whole spine (lower part of C2 to upper part of S1), with a total of 46 anterior vertebral corners for each subject.

Syndesmophytes were defined as a modified Stoke Ankylosing Spondylitis Spine Score (mSASSS) (21) of 2 or 3 (Fig. 1), at the anterior corner of the cervical spine (lower part of C2 to upper part of T1) and the lumbar spine (lower part of T12 to upper part of S1) on lateral view of conventional radiographs for a total of 24 anterior vertebral corners for each subject (Fig. 1).

Imaging interpretation

Two rheumatologists who were blinded to the clinical data and 18F-fluoride PET data recorded the presence or absence of CILs on MRI and the syndesmophytes on conventional radiography. Concordant data between the 2 readers were analysed in the present study. Two nuclear physicians who were blinded to the clinical data and the results of MRI interpreted the PET images and recorded the presence or absence of increased 18F-fluoride uptake lesion. In addition, the 18F-fluoride uptake was analysed with the Philips Extended Brilliance Workspace version 4.5.3.40140 (Philips Healthcare, Best, The Netherlands) using the maximum standardised uptake value (SUVmax). A volume of interest was drawn on the axial plane of the anterior corner of each vertebral body.

Statistical analysis

Data were summarised as the mean (±standard deviation [SD]) or median (inter-quartile range) for continuous variables, and a number (percentage) for categorical variables, as appropriate. For group comparisons, the Mann-Whitney U-test or the Kruskal-Wallis test with Dunn's procedure for *post hoc* evaluation was used to compare continuous variables and the chi-squared test or Fisher's exact test was performed for categorical variables, as appropriate. The primary interest of our study was to investigate whether the presence of CIL (spinal inflam-

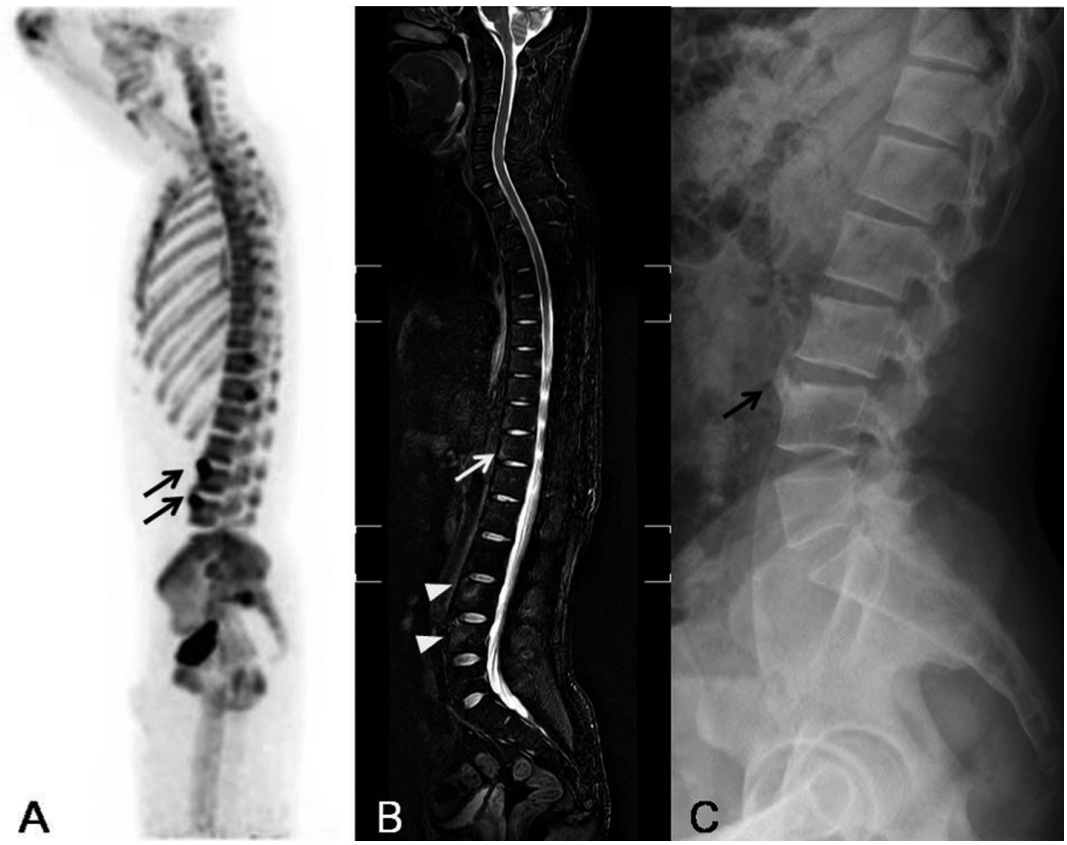

Fig. 1. **A** 42-year-old male patient with ankylosing spondylitis.
A. 18F-fluoride positron emission tomography scan shows increased 18F-fluoride uptake in the anterior vertebral corner of the upper L4 and L5 (arrows).
B. Short tau inversion recovery magnetic resonance image shows a type A corner inflammatory lesion at T11 lower (arrow) and type B corner inflammatory lesion at the upper L4 and L5 (arrowheads).
C. Radiograph shows a syndesmophyte at the upper L4 (arrow).

mation) or syndesmophyte (existing new bone formation) is linked with increased 18F-fluoride uptake lesion to at the vertebral corner level. Statistical association was calculated as odds ratio (OR) with 95% confidence intervals using generalised linear latent and mixed model (GLLAMM) adjusting for within-patient dependence for the total number of anterior vertebral corner (20, 22). *p*-values less than 0.05 were considered statistically significant. All statistical analyses were performed using STATA 11.1 for Windows (StataCorp LP, College Station, TX, USA) and GraphPad prism 5.0 (GraphPad software, CA, USA).

Results

Table I summarises the clinical characteristics of study subjects. The mean (±SD) age and the median (IQR) disease duration were 38.2 (±8.3) years and 42 (32–42.8) months, respectively. The median (IQR) BASDAI score was 3.45 (1.16–5.95). All patients with AS were treated with NSAIDs and sulfasalazine and 1 patient was receiving methotrexate.

As shown in Table II, for patient level, the median (IQR) number of type A and B CIL, syndesmophytes and increased number of 18F-fluoride uptake lesions were 4 (2–7.5), 3 (0.25–5.75), 3 (1–7.5) and 4.5 (1.5–8.75), respectively. At the anterior vertebral corner level, there were 67 type A CILs (12.1%), 37 type B CILs (6.7%) and 58 increased 18F-fluoride uptake lesions (10.4%) out of 552 vertebral anterior corners (C2 lower to S1 upper) and there were 57 syndesmophytes (19.8%) out of 288 vertebral anterior corners (C2 lower to T1 upper and T12 lower to S1 upper). There were no CILs or syndesmophytes or increased 18F-fluoride uptake lesions in the spine of the 33 year-old healthy male volunteer.

A comparison of SUVmax of the 18F-fluoride uptake in the anterior vertebral corner according to the presence or absence of CILs and syndesmophyte is shown in Figure 2. There was a sig-

Table I. Baseline demographics of 12 male patients with ankylosing spondylitis.

Variables	Results
Age, years, mean± SD	38.2 ± 8.3
Disease duration, months, median (IQR)	42 (32-42.8)
ESR, mm/hr, median (IQR)	13 (5.8-20)
CRP, mg/dL, median (IQR)	0.33 (0.06-0.6)
BASDAI, median (IQR)	3.45 (1.16-5.95)
BASMI, median (IQR)	2.8 (1.3-4.4)
BASFI, median (IQR)	2.4 (0.7-3.8)
Current medication	
NSAIDs, n (%)	12 (100)
Sulfasalazine, n (%)	12 (100)
Methotrexate, n (%)	1 (8)

ESR: erythrocyte sedimentation rate; CRP: C-reactive protein; BADAI: Bath Ankylosing Spondylitis Disease Activity Index; BASMI: Bath Ankylosing Spondylitis Metrology Index; BASFI: Bath Ankylosing Spondylitis Functional Index; NSAIDs: non-steroidal anti-inflammatory drugs.

Table II. Number of increased 18F-fluoride uptake lesion, corner inflammatory lesion and syndesmophyte.

Patient level	Results
Number of increased 18F-fluoride uptake lesion, median (IQR)	4.5 (1.5-8.75)
Number of type A CIL, median (IQR)	4 (2-7.5)
Number of type B CIL, median (IQR)	3 (0.25-5.75)
Number of syndesmophyte, median (IQR)	3 (1-7.5)
Anterior vertebral corner level	
Increased 18F-fluoride uptake lesion, n (%)	58 (10.4)
Type A CIL, n (%)	67 (12.1)
Type B CIL, n (%)	37 (6.7)
Syndesmophyte, n (%)	57 (19.8)

CIL: corner inflammatory lesion.

nificant difference in SUVmax among no CILs, type A CILs and type B CILs (p<0.001) using the Kruskal-Wallis test. In multiple comparisons, the median SUVmax of the 18F-fluoride uptake in both type A (6.8 [5.7–8.3], p<0.05) and type B CILs (10.6 [8.6–15], p<0.05) was significantly higher than that of the absence of CILs (6.3 [5.6–7.1]). Of interest, type B CILs had a significantly higher SUVmax than type A CILs (p<0.05). The anterior vertebral corner with syndesmophytes showed a significantly higher median SUVmax than that without this feature (6.8 [5.8-7.8] *vs*. 6.3 [5.6-7.1], p=0.025). The mean (±SD) of the SUVmax of the 18F-fluoride uptake in the 46 anterior vertebral corners of the healthy volunteer was 5.6 (±0.8).

Table III shows the frequency of increased 18F-fluoride uptake lesions according to the presence or absence of CILs or syndesmophytes. The anterior vertebral corner that showed type A and B CILs on MRI and syndesmophytes on radiography had a significantly higher frequency of having increased 18F-fluoride uptake on PET than the anterior vertebral corners without these features. Of note, a majority of anterior vertebral corners with type B CILs (75.7%) had increased 18F-fluoride uptake lesions whereas 76.1% of type A CILs and 80.7% of syndesmophyte showed no increased 18F-fluoride uptake lesions.

As shown in Table IV, we performed GLLAMM, including an increased 18F-fluoride uptake lesion as an dependent variable and CILs or syndesmophytes as independent variables adjusting within-patient dependence for the total number of anterior vertebral corners. A type A CIL (OR=3.2, 95% CI=1.6–6.5, p=0.001), type B CIL (OR=59.9, 95% CI=23.5–151.5, p<0.001) and syndesmophyte (OR=21.8, 95% CI=5.5–85.2, p<0.001) were significantly associated with an increased 18F-fluoride uptake lesion.

Discussion

In the present study, the anterior vertebral corners with CILs and syndesmophytes had a significantly higher SUVmax of the 18F-fluoride uptake than those without either features. In addition, GLLAMM models showed that both CIL and syndesmophyte were significantly associated with increased 18F-fluoride uptake lesion after adjusting within-patient dependence for the total number of anterior vertebral corners. This finding suggests that inflammation as well as the existence of new bone formation (syndesmophytes) is linked with increased osteoblastic bone synthesis in the spine of AS patients. Interestingly, type B CILs had a significantly higher SUVmax than type A CILs and most type B CILs (75.7%) had increased 18F-fluoride uptake. Otherwise, a large proportion of type A CILs (76.1%) and syndesmophytes (80.7%) did not have an increased 18F-fluoride uptake lesion, indicating

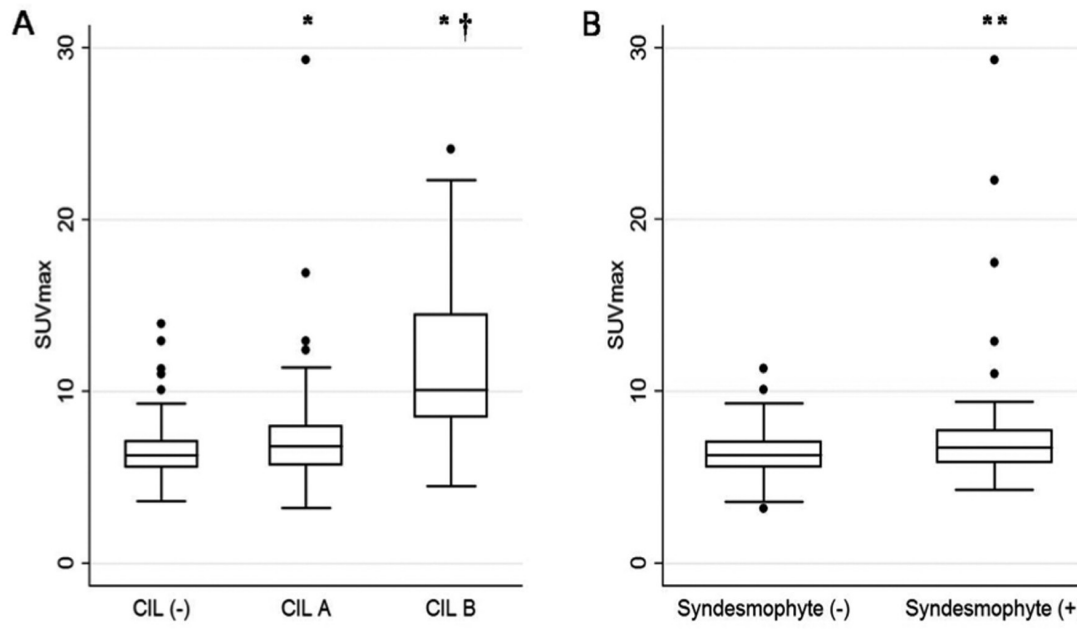

Fig. 2. A. A comparison of the maximum standardised uptake value (SUVmax) of 18F-fluoride uptake in the no corner inflammatory lesions (CILs), type A CILs and type B CILs. *p<0.05 *vs*. no CIL. †p<0.05 *vs*. type A CIL.
B. A comparison of SUVmax of 18F-fluoride uptake according to the presence or absence of syndesmophytes. **p=0.025 *vs*. no syndesmophyte.

Table III. Frequency of increased 18F-fluoride uptake lesion according to the presence or absence of corner inflammatory lesion and syndesmophyte.

	Increased 18F-fluoride uptake lesion		
	Yes	No	*p*-value
Vertebral corner with type A CIL, n (%)	16 (23.9)	51 (76.1)	0.001
Vertebral corner without type A CIL, n (%)	42 (8.7)	443 (91.3)	
Vertebral corner with type B CIL, n (%)	28 (75.7)	9 (24.3)	<0.001
Vertebral corner without type B CIL, n (%)	30 (5.8)	485 (94.2)	
Vertebral corner with syndesmophyte, n (%)	11 (19.3)	46 (80.7)	<0.001
Vertebral corner without syndesmophyte, n (%)	6 (2.6)	225 (97.4)	

CIL: corner inflammatory lesion.

Table IV. Generalised linear latent and mixed model for evaluating the association of increased 18F-fluoride uptake lesion with corner inflammatory lesion and syndesmophyte.

Variables	OR (95% CI)	*p*-value
Type A CIL	3.2 (1.6-6.5)	0.001
Type B CIL	59.9 (23.5-151.5)	<0.001
Syndesmophyte	21.8 (5.5-85.2)	<0.001

CIL: corner inflammatory lesion.

that not all type A CILs and syndesmophytes showed active bone synthesis. Additionally, type B CIL had a higher OR for the presence of increased 18F-fluoride uptake lesion than type A CIL or syndesmophyte. Therefore, osteoblastic activity in the anterior vertebral corners of patients with AS was obviously increased in type B CILs, whereas type A CILs and syndesmophytes showed a somewhat weaker association with active bone synthesis.

The pathogenesis of the structural damage in AS is not fully understood. "Early" inflammatory lesions of the spine in AS are driven by proinflammatory cytokines such as TNF-α; these lesions can progress to "mature" inflammatory lesions reflecting postinflammatory tissue metaplasia. In established mature lesions, the reparative process leads to new bone formation activated through bone morphogenic protein (BMP) and the Wingless and INT-1 (WNT) signaling pathway, which are inhibited by DKK-1 and sclerostin. The inflammation can trigger osteoproliferation induced by BMP and the WNT pathway, whereas TNF-α also upregulates DKK-1. Once inflammation resolves either spontaneously or through pharmacological suppression of TNF-α, this downregulates DKK-1 and, in turn, enhances BMP and the WNT pathway to promote new bone formation. Thus, TNF-α can act as a brake on new bone formation. This process is termed as the "TNF brake hypothesis" by Maksymowich, suggesting a link between inflammation and new bone formation (9). Clinical trials that have shown that using anti-TNF-α agents for 2 years fails to prevent new bone formation despite the dramatic improvement of inflammation support this notion (1-3). In addition, a recent longitudinal study reported that resolution of inflammation in more advanced lesions (type B CIL) rather than type A CIL is associated with the development of new syndesmophytes, supporting evidence for the TNF brake hypothesis (20). In line with previous results, type B CILs showed more active osteoproliferation than type A CILs as assessed by uptake of 18F-fluoride tracer on PET imaging in our study. Thus, we assumed that the type B CILs represent the spot of highly active bone synthesis which is an important "checkpoint" or "brake" in the course of structural damage in AS similar to the process of the TNF brake hypothesis. However, it is beyond the scope of our study to prove the TNF brake hypothesis and further longitudinal research is obviously needed.

Contrary to the TNF brake hypothesis, some dissociation between inflammation and new bone formation has been suggested. Some studies have shown that the large majority of new syndesmophytes develop in vertebral corners in the absence of inflammation (4, 6) and Baralikaos *et al*. argued that the sequence of inflammation-fat degeneration-new bone formation was rarely observed (23). Thus, new bone formation in AS patients may be induced by a non-inflammatory process. Lories *et al*. suggested that inflammation and the triggering of skeletal progenitor cells leading to new bone formation and ankylosis are initiated and propagated simultaneously, not sequentially, by entheseal stress as the primary event of AS (24). This notion is termed as the "alternative hypothesis". Of note, a majority of type A CILs (76.1%) and syndesmophytes (80.7%) did not show an increased 18F-fluoride uptake lesion in the present study (Table II), which is consistent with the alternative hypothesis to some degree.

The 18F-fluoride isotope is incorporated into the bone structure at the sites of active osteoblastic bone formation during bone remodeling or tissue repair and is therefore considered as bone-specific tracer (17). An increased 18F-fluoride uptake lesion in the skeleton reflects increased blood flow as well as increased regional metabolic activity of bone (14, 25, 26). In addition, the 18F-fluoride PET scan has a higher spatial resolution and better bone-soft tissue contrast ratio than that of 99mTc-methyldiphosphonate based on bone scintigraphy. Therefore, the 18F-fluoride PET scan can provide excellent imaging quality and high sensitivity in evaluating bone metabolism (14). To date, there have been 3 studies assessing the axial skeleton in AS patients using 18F-fluoride PET scan. Strobel *et al*. reported a potential diagnostic role of the 18F-fluoride PET-computed tomography (CT) in the detection of sacroiliitis in AS patients (27) and Bruijen *et al*. showed increased bone formation in the spine of 2 patients with AS using the 18F-fluoride PET-CT scan (16). However, these studies did not systematically evaluate the spine of AS patients. Recently, Fischer *et al*. demonstrated that 18F-fluoride uptake in the PET/CT is

modestly associated with an inflammatory lesion on MRI in 10 patients with AS (28). There are several differences in methodological aspects between the study by Fischer *et al*. and that of ours. Firstly, Fischer *et al*. did not compare data of the PET/CT with conventional radiography. Secondly, Fischer *et al*. used the kappa value for evaluating the relationship between increased 18F-fluoride uptake and inflammatory lesion on MRI and did not adjust within-patient dependence for the total number of anterior vertebral corners. Thus, our GLLAMM can provide statistical association that is more accurate. Lastly, the PET-MRI which can scan both PET and MRI simultaneously was used in our study. In the aspect of detecting active bone formation, the 18F-fluoride PET scan has a potential role for evaluating structural damage in patients with AS.

The present study definitely has some limitations. First, due to cross-sectional design, we did not evaluate the association between bone synthetic activity demonstrated in the 18F-fluoride PET and the future development of syndesmophytes. This warrants a longitudinal study evaluating the structural damage using the 18F-fluoride tracer. Second, increased 18F-fluoride uptake lesion in patients with AS should be interpreted cautiously because of lack of further data on the spine with AS using the 18F-fluoride PET scan. Previous studies have shown that 18F-fluoride uptake was also observed in the spine of subjects with various musculoskeletal disorders including spondylosis, fracture, osteoid osteoma and herniated disk (29, 30). Thus, degenerative change such as osteophytes in the spine of AS patients may also show an increased 18F-fluoride uptake and complicate the interpretation of our results. In addition, the definition of an increased 18F-fluoride uptake lesion was somewhat arbitrary and it varies between studies. Standardising the definition of increased 18F-fluoride uptake lesion is needed for evaluating the axial skeleton of patients with AS. Likewise, SUVmax of the 18F-fluoride should be reported with major caution. A segmentation-based attenuation correction method is adopted in PET-MRI system, which is regarded as more reliable than template-guided attenuation correction method (31). The segmentation algorithm attempts to distinguish three biological classes: air, lung and soft tissue, however, has a difficulty in distinguishing bone and air intensities in MRI (32). Thirdly, AS patients in our study were treated with NSAIDs and sulfasalazine and had disease duration up to 8 years. Although NSAIDs are reported to slow the radiographic progression of AS (33, 34), we could not fully adjust the effect of these medications in the 18F-fluoride uptake. Discontinuation of NSAIDs before participation in our study was not considered due to the ethical issue. Additionally, considering the positive relationship between disease duration and radiographic change in AS (35), the heterogeneity in disease duration was another limitation of this study.

In summary, both CILs and syndesmophytes were associated with increased osteoblastic bone synthesis when assessed according to 18F-fluoride uptake. Among them, type B CILs, the advanced inflammatory lesions showed more active osteoblastic activity than type A CILs, the early and active inflammatory lesions or syndesmophytes, the existence of new bone formation. 18F-fluoride PET-MRI may have potential for investigating the relationship between new bone formation and inflammation in AS patients.

References

1. VAN DER HEIJDE D, LANDEWÉ R, EINSTEIN S *et al*.: Radiographic progression of ankylosing spondylitis after up to two years of treatment with etanercept. *Arthritis Rheum* 2008; 58: 1324-31.
2. VAN DER HEIJDE D, LANDEWÉ R, BARALIAKOS X *et al*.: Radiographic findings following two years of infliximab therapy in patients with ankylosing spondylitis. *Arthritis Rheum* 2008; 58: 3063-70.
3. VAN DER HEIJDE D, SALONEN D, WEISSMAN BN *et al*.: Assessment of radiographic progression in the spines of patients with ankylosing spondylitis treated with adalimumab for up to 2 years. *Arthritis Res Ther* 2009; 11: R127.
4. BARALIAKOS X, LISTING J, RUDWALEIT M, SIEPER J, BRAUN J: The relationship between inflammation and new bone formation in patients with ankylosing spondylitis. *Arthritis Res Ther* 2008; 10: R104.
5. MAKSYMOWYCH WP, CHIOWCHANWISAWAKIT P, CLARE T, PEDERSEN SJ, OSTERGAARD M, LAMBERT RG: Inflammatory lesions of the spine on magnetic resonance imaging predict the development of new syndesmophytes in ankylosing spondylitis: evidence of a relationship between inflammation and new bone formation. *Arthritis Rheum* 2009; 60: 93-102.
6. VAN DER HEIJDE D, MACHADO P, BRAUN J *et al*.: MRI inflammation at the vertebral unit only marginally predicts new syndesmophyte formation: a multilevel analysis in patients with ankylosing spondylitis. *Ann Rheum Dis* 2012; 71: 369-73.
7. SIEPER J, APPEL H, BRAUN J, RUDWALEIT M: Critical appraisal of assessment of structural damage in ankylosing spondylitis: implications for treatment outcomes. *Arthritis Rheum* 2008; 58: 649-56.
8. LORIES RJ, SCHETT G: Pathophysiology of new bone formation and ankylosis in spondyloarthritis. *Rheum Dis Clin North Am* 2012; 38: 555-67.
9. MAKSYMOWYCH WP: Disease modification in ankylosing spondylitis. *Nat Rev Rheumatol* 2010; 6: 75-81.
10. BRAUN J, BARALIAKOS X: Imaging of axial spondyloarthritis including ankylosing spondylitis. *Ann Rheum Dis* 2011; 70 (Suppl. 1): i97-103.
11. CARMONA L, SELLAS A, RODRIGUEZ-LOZANO C *et al*.: Scoring with the Berlin MRI method for assessment of spinal inflammatory activity in patients with ankylosing spondylitis: a calibration exercise among rheumatologists. *Clin Exp Rheumatol* 2013; 31: 883-8.
12. APPEL H, LODDENKEMPER C, GROZDANOVIC Z *et al*.: Correlation of histopathological findings and magnetic resonance imaging in the spine of patients with ankylosing spondylitis. *Arthritis Res Ther* 2006; 8: R143.
13. SIEPER J, RUDWALEIT M, BARALIAKOS X *et al*.: The Assessment of SpondyloArthritis international Society (ASAS) handbook: a guide to assess spondyloarthritis. *Ann Rheum Dis* 2009; 68 (Suppl. 2): ii1-44.
14. LI Y, SCHIEPERS C, LAKE R, DADPARVAR S, BERENJI GR: Clinical utility of (18)F-fluoride PET/CT in benign and malignant bone diseases. *Bone* 2012; 50: 128-39.
15. HSU WK, VIRK MS, FEELEY BT, STOUT DB, CHATZIIOANNOU AF, LIEBERMAN JR: Characterization of osteolytic, osteoblastic, and mixed lesions in a prostate cancer mouse model using 18F-FDG and 18F-fluoride PET/CT. *J Nucl Med* 2008; 49: 414-21.
16. BRUIJNEN ST, VAN DER WEIJDEN MA, KLEIN JP *et al*.: Bone formation rather than inflammation reflects ankylosing spondylitis activity on PET-CT: a pilot study. *Arthritis Res Ther* 2012; 14: R71.
17. TAN AL, TANNER SF, WALLER ML *et al*.: High-resolution [18F]fluoride positron emission tomography of the distal interphalangeal joint in psoriatic arthritis--a bone-enthesis-nail complex. *Rheumatology* (Oxford) 2013; 52: 898-904.
18. VAN DER LINDEN S, VALKENBURG HA, CATS A: Evaluation of diagnostic criteria for ankylosing spondylitis. A proposal for modification of the New York criteria. *Arthritis Rheum* 1984; 27: 361-8.
19. LAMBERT RGW, PEDERSEN SJ, MAKSY-

MOWYCH WP, CHIOWCHANWISAWAKIT P, OSTERGAARD M: Active inflammatory lesions detected by magnetic resonance imaging in the spine of patients with spondyloarthritis - definitions, assessment system, and reference image set. *J Rheumatol Supplement* 2009; 84: 3-17.

20. MAKSYMOWYCH WP, MORENCY N, CONNER-SPADY B, LAMBERT RG: Suppression of inflammation and effects on new bone formation in ankylosing spondylitis: evidence for a window of opportunity in disease modification. *Ann Rheum Dis* 2013; 72: 23-8.
21. WANDERS AJ, LANDEWÉ RB, SPOORENBERG A *et al*.: What is the most appropriate radiologic scoring method for ankylosing spondylitis? A comparison of the available methods based on the Outcome Measures in Rheumatology Clinical Trials filter. *Arthritis Rheum* 2004; 50: 2622-32.
22. CHIOWCHANWISAWAKIT P, LAMBERT RG, CONNER-SPADY B, MAKSYMOWYCH WP: Focal fat lesions at vertebral corners on magnetic resonance imaging predict the development of new syndesmophytes in ankylosing spondylitis. *Arthritis Rheum* 2011; 63: 2215-25.
23. BARALIAKOS X, HELDMANN F, CALLHOFF J *et al*.: Which spinal lesions are associated with new bone formation in patients with ankylosing spondylitis treated with anti-TNF agents? A long-term observational study using MRI and conventional radiography. *Ann Rheum Dis*. 2013.
24. LORIES RJ, LUYTEN FP, DE VLAM K: Progress in spondylarthritis. Mechanisms of new bone formation in spondyloarthritis. *Arthritis Res Ther* 2009; 11: 221.
25. MESSA C, GOODMAN WG, HOH CK *et al*.: Bone metabolic activity measured with positron emission tomography and [18F]fluoride ion in renal osteodystrophy: correlation with bone histomorphometry. *J Clin Endocrinol Metab* 1993; 77: 949-55.
26. PIERT M, ZITTEL TT, BECKER GA *et al*.: Assessment of porcine bone metabolism by dynamic. *J Nucl Med* 2001; 42: 1091-100.
27. STROBEL K, FISCHER DR, TAMBORRINI G *et al*.: 18F-fluoride PET/CT for detection of sacroiliitis in ankylosing spondylitis. *Eur J Nucl Med Mol Imaging* 2010; 37: 1760-5.
28. FISCHER DR, PFIRRMANN CW, ZUBLER V *et al*.: High bone turnover assessed by 18F-fluoride PET/CT in the spine and sacroiliac joints of patients with ankylosing spondylitis: comparison with inflammatory lesions detected by whole body MRI. *EJNMMI Res* 2012; 2: 38.
29. OVADIA D, METSER U, LIEVSHITZ G, YANIV M, WIENTROUB S, EVEN-SAPIR E: Back pain in adolescents: assessment with integrated 18F-fluoride positron-emission tomography-computed tomography. *J Pediatr Orthop* 2007; 27: 90-3.
30. LIM R, FAHEY FH, DRUBACH LA, CONNOLLY LP, TREVES ST: Early experience with fluorine-18 sodium fluoride bone PET in young patients with back pain. *J Pediatr Orthop* 2007; 27: 277-82.
31. KIM JH, LEE JS, SONG IC, LEE DS: Comparison of segmentation-based attenuation correction methods for PET/MRI: evaluation of bone and liver standardized uptake value with oncologic PET/CT data. *J Nucl Med* 2012; 53: 1878-82.
32. SCHULZ V, TORRES-ESPALLARDO I, RENISCH S *et al*.: Automatic, three-segment, MR-based attenuation correction for whole-body PET/MR data. *Eur J Nucl Med Mol Imaging* 2011; 38: 138-52.
33. WANDERS A, HEIJDE D, LANDEWÉ R *et al*.: Non-steroidal anti-inflammatory drugs reduce radiographic progression in patients with ankylosing spondylitis: a randomized clinical trial. *Arthritis Rheum* 2005; 52: 1756-65.
34. KROON F, LANDEWÉ R, DOUGADOS M, VAN DER HEIJDE D: Continuous NSAID use reverts the effects of inflammation on radiographic progression in patients with ankylosing spondylitis. *Ann Rheum Dis* 2012; 71: 1623-9.
35. DORAN MF, BROPHY S, MACKAY K, TAYLOR G, CALIN A: Predictors of longterm outcome in ankylosing spondylitis. *J Rheumatol* 2003; 30: 316-20.